

Charles A. Knight\*, Robert A. Rilling, and L. Jay Miller  
National Center for Atmospheric Research, Boulder, Colorado

## 1. INTRODUCTION

The NCAR S-Pol radar was operated in RICO (Rain In Cumulus over the Ocean) during Nov.-Jan. 2004-05, as part of a study of trade-wind cumulus clouds. Project objectives ranged from understanding the microphysical mechanism of rain formation and evaluating the importance of precipitation in trade-wind cumulus, to the larger-scale effects of the clouds. Specific interest in the cloud microphysics centered on understanding the time of onset of coalescence growth of rain drops and on the role of giant and ultra-giant aerosol in raindrop formation. To quote from Malkus (1962; and reinforced by personal communication, Simpson, 2005), "Rainfall in the trade stream is the least reliable of its properties. Even casual observers have noted that a skyful of trade cumuli on some days produces plentiful showers from clouds of all sizes, while on other days with apparently similar cloud conditions no drop of rain appears." This observation poses a scientific problem: an apparent extreme variability of an important aspect of cloud behavior that needs to be explained. If this variability is real, is it a function of the aerosol or some other parameter not apparent to the visual observer? But might it be an artifact of visual observation? Is it also evident on radar, which is a much better way of observing precipitation than the naked eye and, using Bragg scattering with an S-band radar, also a reasonably good way of observing cloud?

Addressing the overall issue raised by the above quotation is one objective of data analysis from the RICO project, and a start at one aspect of it is reported here. We discuss methods for characterizing precipitation formation in these clouds using the dual-polarization, very sensitive S-band (10-cm-wavelength) radar, and present somewhat preliminary results, using values for the equivalent reflectivity factor and  $Z_{DR}$ , the dual polarization ratio.

The radar was on Barbuda, in the Eastern Caribbean. With clouds coming from the East, the only direct land influences are from Barbuda itself, and should be minimal except for clouds either downwind or very close to the island, which, though about 9 km long, is everywhere lower than about 50m above sea level. The S-band radar was operated 24 hours a day for most of the experiment, usually with routine, approximately 180° sectors centered cross-wind, so as to get as many complete cloud histories as possible. Scanning was almost always in PPI mode with six to eight elevation angle steps. A complete volume scan over the sector usually took between 3 and 4 minutes. The averaging

over 50 hits led to noisier reflectivity data than one would have desired, but appears to have been a worthwhile compromise for the sake of spatial and temporal resolution and coverage, in studying trade-wind cumuli. Another radar, Ka-band, with beam matched to the S-band and its antenna co-mounted, was operated about one third of the time. The present paper uses only the S-band data.

More detail on characteristics of the S-Pol radar can be found at <http://www.atd.ucar.edu/rsf/spol/spol.html>.

## 2. ANALYSIS METHODS

The data consist of quasi-horizontal slices of radar echo at 4 to 8 levels through the clouds (usually; a function of range), every 3 to 4 minutes. With very few exceptions, no effort was made to track individual clouds in more detail, because experience had shown that doing this results in consistently missing the earliest times, which are crucial to the microphysical interpretations. For the same reason, the scan elevation angles were almost never altered to maximize coverage on any individual cloud. With this scanning procedure, cloud top heights are not generally recoverable with useful accuracy, but with the 1° beamwidth and using PPIs, cloud top height is poorly resolved anyway.

Special effort is made to track individual precipitation echoes backwards in time, starting from the first precipitation detectable in the lowest-level, 0.5° elevation scan. Many cases are available in the data, and so far the selection has been on the basis of both location and intensity: cases are analyzed for which the first precipitation is close to and preferably downwind of the radar, and the maximum dBZ attained is relatively strong: 30 to 50 dBZ.

Inspection of the data in the field gave two main, preliminary conclusions, both of which have held up in the analysis to date. One is that the trade-wind cumulus clouds, though small (tops usually below about 2.5 km) are very long-lasting, often being trackable on radar for an hour or more. The limit on useful tracking often was imposed by range from the radar. Figure 1 shows one example. The clouds are a succession of more or less discreet updrafts, both visually and on radar. Tracking backwards in time, the earliest stages are tracked with Bragg echo. (Bragg echo can be strong in small cumulus: up to about 10dBZ, in Florida with an S-band radar (Knight and Miller, 1998)). We find that the Bragg-only stage can be lengthy, and that it often involves a considerably bigger area than the early precipitation echo, as if the discrete, relatively narrow

---

\*Corresponding author address: Charles A. Knight, National Center for Atmospheric Research, P.O. Box 3000, Boulder, CO 80307; e-mail: knightc@ucar.edu.

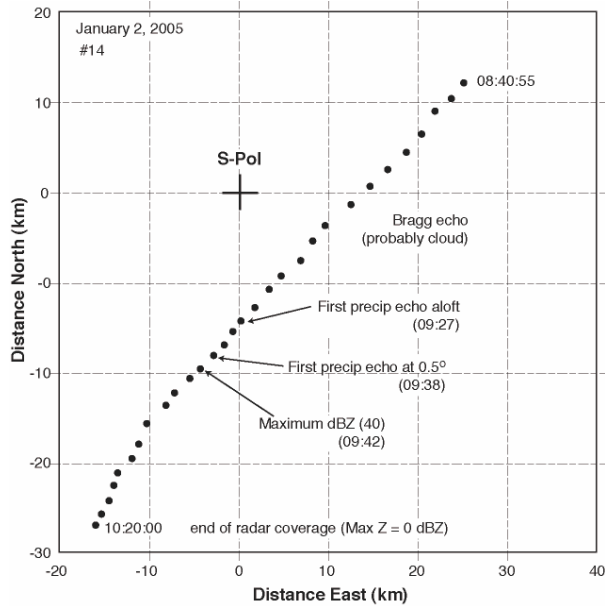


**Fig. 1.** Track of a long-lived trade-wind cumulus that passed about 10 km from the radar. The portion of the track before the first precipitation echo aloft is following a rather ill-defined maximum in Bragg scattering (usually at about 0dBZ) that becomes progressively shallower at earlier times, but is much broader than the precipitation echo. Each dot represents a volume scan.

updraft that leads to the first detectable precipitation formation often originates within broader, shallower cloud. The second conclusion was that the  $Z_{DR}$  values in general were unexpectedly low. The radar echoes are dominated nearly all the time by large concentrations of drizzle, not small concentrations of large drops.

How should the precipitation from these small cumuli be characterized, using dBZ and  $Z_{DR}$ ? Time-height diagrams of dBZ have usually represented maximum values as a function of height, perhaps so as to reflect cloud or storm intensity, but that is clearly inappropriate for these small cumulus. For one thing, the maximum values of dBZ and of  $Z_{DR}$  often do not coincide in space. This indicates, not surprisingly, that the drop size distributions can vary a great deal within single PPI slices through a cloud. Figure 2 shows a rather extreme example, probably due to size sorting, but such are not uncommon. We chose to estimate dBZ and  $Z_{DR}$  over whole, PPI sweeps, to get a measure of overall size distribution at each time and level, producing time-height plots of “total” dBZ and  $Z_{DR}$  that we will label TdBZ and TZ $_{DR}$ . Thus, single values for the constant-elevation-angle sweeps through cloud, for TdBZ and TZ $_{DR}$  are calculated according to

$$TdBZ = 10 \log \left( \frac{\sum Z_{HH}}{\#} \right)$$

and

$$TZ_{DR} = 10 \log \left( \frac{\sum Z_{HH} / \sum Z_{VV}}{\#} \right)$$

where the sums are over all of the in-cloud pulse volumes in the entire sweep,  $Z$  is the equivalent radar reflectivity factor,  $H$  and  $V$  represent horizontally and vertically polarized transmission and reception, and  $\#$  is the number of data points in the sum.

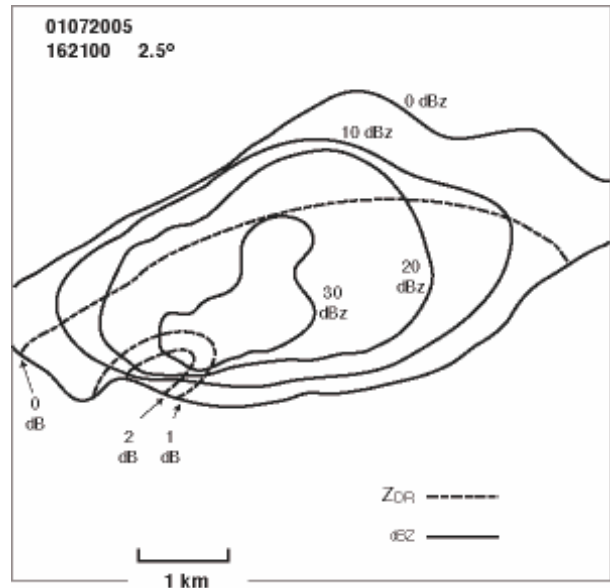


**Fig. 2.** Solid contours of dBZ, from 0 to 30dBZ show a well-defined maximum, as do the dashed contours of  $Z_{DR}$  from 0 to 2dB, but the two maxima do not coincide. The PPI from which this was drawn is in Fig. 7, below.

### 3. RESULTS AND DISCUSSION

Much cloud physical thought about how coalescence is able to start so fast has been stimulated by reported times of 20 to 30 minutes to precipitation formation in small, warm cumulus, (e.g., Saunders, 1965). Visual and radar data were gathered in RICO with the hope of being able to document this kind of information better than has been done in the past. While that effort probably was quite successful operationally, the long tracking times illustrated in Fig. 1, with long periods of tracking Bragg scattering echoes, suggest that a simple number of minutes to precipitation “onset” that can be applied to a cloud parcel starting from initial condensation, so as to test the early coalescence rates, may never be forthcoming from this kind of observation. Whole-cloud models that are quite faithful to detailed observation in the very early stages of cloud formation will probably be needed to determine whether there is or is not a physical problem in understanding how fast coalescence starts in these clouds.

In studying precipitation, we wish to be sure to eliminate as much of the Bragg scattering component as possible. To do that, the radar data are thresholded on  $dBZ_{HH}$ , testing two thresholds, -1 and 9 dB. These were hand-calculated by first calculating  $Z_{HH}$  and  $Z_{VV}$  from available values of dBZ and  $Z_{DR}$  in 2.0 and 0.2dB bins

(respectively), centered at 0, 2, 4, ... and ..., -0.2, 0, +0.2, ... dB. ( $Z_{HH}$  is binned, but the resulting  $Z_{VV}$  values are not.)

Before presenting time-height plots, Fig. 3 shows scatter plots of  $Z_{DR}$  vs. dBZ, from one volume scan in Fig. 4. The trend of decreasing scatter of  $Z_{DR}$  vs dBZ as height increases shown in Fig. 3 is a general feature of the data so far examined. There is no evident side lobe contamination from sea clutter in the data over the ocean, and we do not have a firm explanation for this trend. The frigate bird colony on Barbuda provided a plentiful source of bird echoes in surface convergence regions and apparently sometimes also within cloud, but they appear to be easily identifiable by anomalous velocity and  $Z_{DR}$  values, and probably do not account for the scatter.

The one case illustrated in Fig. 4 shows very low values of  $TZ_{DR}$  accompanying TdBZ to 20dBZ, which include maximum dBZ values to 30dBZ. Illingworth (1988) reported just the opposite: large values of  $Z_{DR}$  in the early echo of small cumulus in Georgia. Figure 5 is a schematic of his results from that paper, including a curve for "average rainfall," a Marshall-Palmer distribution with  $N_0 = 8000 \text{ m}^{-3} \text{ mm}^{-1}$ . The results of Fig. 4 are added into Fig. 5, represented by the steep dashed line to the left. While Illingworth concluded from his data that the early rainfall consisted of small concentrations of several-millimeter-sized water drops, obviously the conclusion here is the opposite: that the early rainfall, in fact all the rainfall in this case, is dominated by small drops, with a dearth, not a surplus,

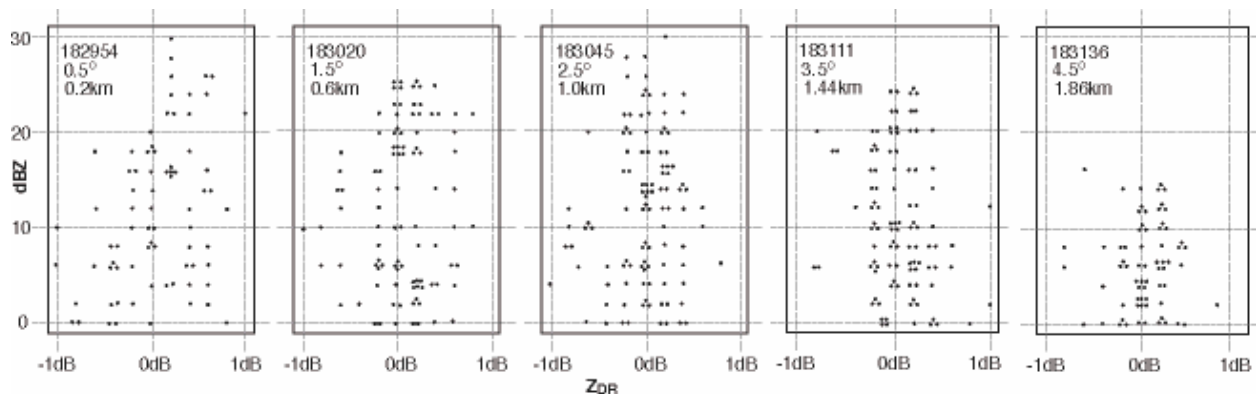


**Fig. 3.** Scatter plots of  $Z_{DR}$  vs. dBZ from one volume scan of Fig. 4. Note that the mean  $Z_{DR}$  is always close to 0dB, and that the scatter decreases with height but does not depend strongly upon dBZ. This cloud is not the same one used for either Fig. 1 or Fig. 2.

Figures 4a and 4b show time-height plots of TdBZ vs.  $TZ_{DR}$  using thresholds of 9dBZ (a) and -1dBZ (b). Figure 4c gives both the number of radar data points that contribute to each value (the numbers given are for the -1dBZ threshold) and the maximum dBZ that would have been plotted in a conventional dBZ time-height diagram. In Figure 4, the thresholding at 9dBZ is the safest in terms of being sure to eliminate nearly all of the Bragg scattering influence, but in many instances it will also eliminate a lot of echo that is from cloud droplets. We think that the thresholding at -1dB is probably more realistic in representing precipitation production, but it makes little difference in terms of the overall conclusions drawn in this paper. Comparison of the values with the two thresholds shows that while including Z values between -1 and 9dBZ may make an appreciable difference in the TdBZ values, it makes rather little difference to the overall  $TZ_{DR}$ , even when TdBZ with the -1dBZ threshold is very weak. (Note that at the range of the cloud in Figs. 3 and 4, about 23 km, the radar noise level is below -20dBZ.) Figure 4c shows that the maximum dBZ in a PPI slice is about 10dB above TdBZ at the higher numerical values in this case. The areal extent of a single radar data "point" at this range is about  $0.05 \text{ km}^2$ .

of several-millimeter raindrops compared to the representation of average rainfall. (For rain with uniform-sized drops, 0.2 dB  $Z_{DR}$  corresponds roughly to 1mm diameter). The data treatments are different, in that Illingworth averaged the  $Z_{DR}$  for each 2 dBZ interval to obtain his separate points, while we average both reflectivity factor and  $Z_{DR}$  over entire PPI slices through the cloud for our data points, but it is evident from the scatter plots in Fig. 3 that using his way of treating the data would not change the great difference between the two sets of results.

Included in Fig.5 also are data from one RHI scan in Florida (shown in Fig. 6, from a case in Knight et al. (2002)). The data were stratified in 500m height intervals and averaged using the equations above, like the RICO data. The numbers at each point are the total number of pulse volumes in each, a -1dBZ threshold on Z was used, and the lowest level where the echo was dominated by insects was not included. The radar scan (Fig. 6) shows extreme size sorting, with the big drops falling out earliest, as was typical in the early echoes in the Florida clouds.

The Florida data are more in agreement with Illingworth's results than with the RICO data. At this point one might look for explanation of these differences either in the probably much more maritime aerosol in

RICO or in different cloud dynamics, in that the RICO clouds may have weaker updrafts that build up more slowly.

We plan to generalize the RICO analysis over the entire data set, and if there is significant variability of behavior of  $Z_{DR}$  vs. dBZ, look for correlations that may explain it. Experience from hand-analysing much of the data presented here, along with inspection of more cases, suggests that the present results will represent the general rule for the maritime, trade-wind cumulus observed in RICO.

#### REFERENCES

Illingworth, A. J., 1988: The formation of rain in convective clouds. *Nature*, **336**, 754-756.

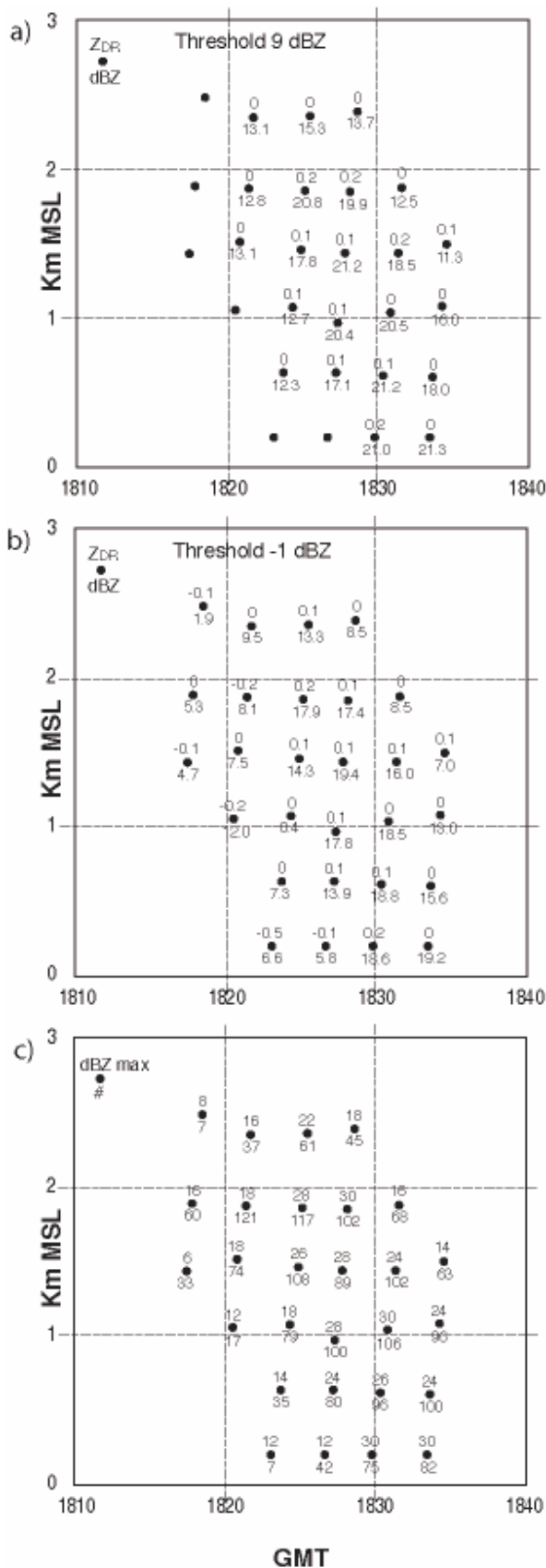
Knight, C.A. and L. J. Miller, 1998: Early radar echoes from small, warm cumulus: Bragg and hydrometeor scattering. *J. Atmos. Sci.*, **55**, 2974-2992.

Knight, C. A., J. Vivekanandan, and S. G. Lasher-Trapp, 2002: First radar echoes and the early ZDR history of Florida cumulus. *J. Atmos. Sci.*, **59**, 1454-1472.

Malkus, J. S., 1962: Large-scale interactions, in *The Sea*, Vol. 1, M. N. Hill, Ed. (Interscience, New York) pp. 88-294.

Saunders, P. M., 1965: Some characteristics of tropical marine showers. *J. Atmos. Sci.*, **22**, 167-175.

**Fig. 4.** Time-height representations of data for a precipitation echo on Jan. 7, 2005. Dots represent the location of data points, and in a) and b) the numbers above and below each dot are the overall  $Z_{DR}$  ( $TZ_{DR}$ , to the nearest 0.1dB) and TdBZ, defined in the text. In a), the threshold is 9dBZ and in b), -1dBZ. In c) the upper number is the maximum dBZ in the cloud at that height, and the lower number is the number of data points that contributed to each value in Fig. 4b. The PPI for the point at about 1826, 1.9 km, with  $TZ_{DR}$  0.2 dB, is given in Fig. 8.



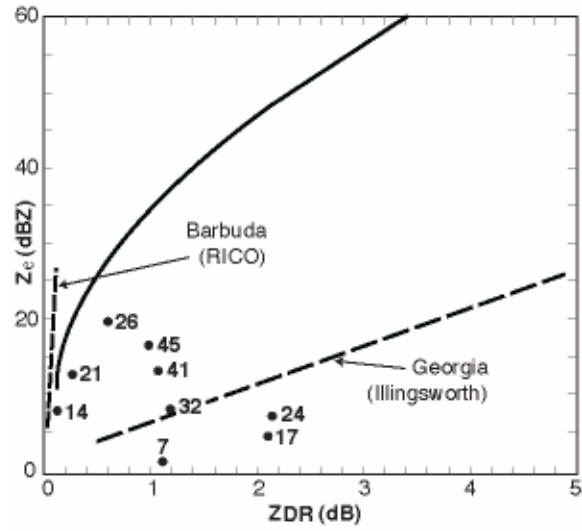


**Fig. 5.** Plot of  $Z$  vs  $Z_{DR}$ , after Illingsworth (1988) in which the solid line represents average rainfall and the dashed lines represent the locations of his data and the present data, as labeled. The single points are from a Florida case in 1998 (see text), averages from constant height slabs of the RHI shown in Fig. 6.

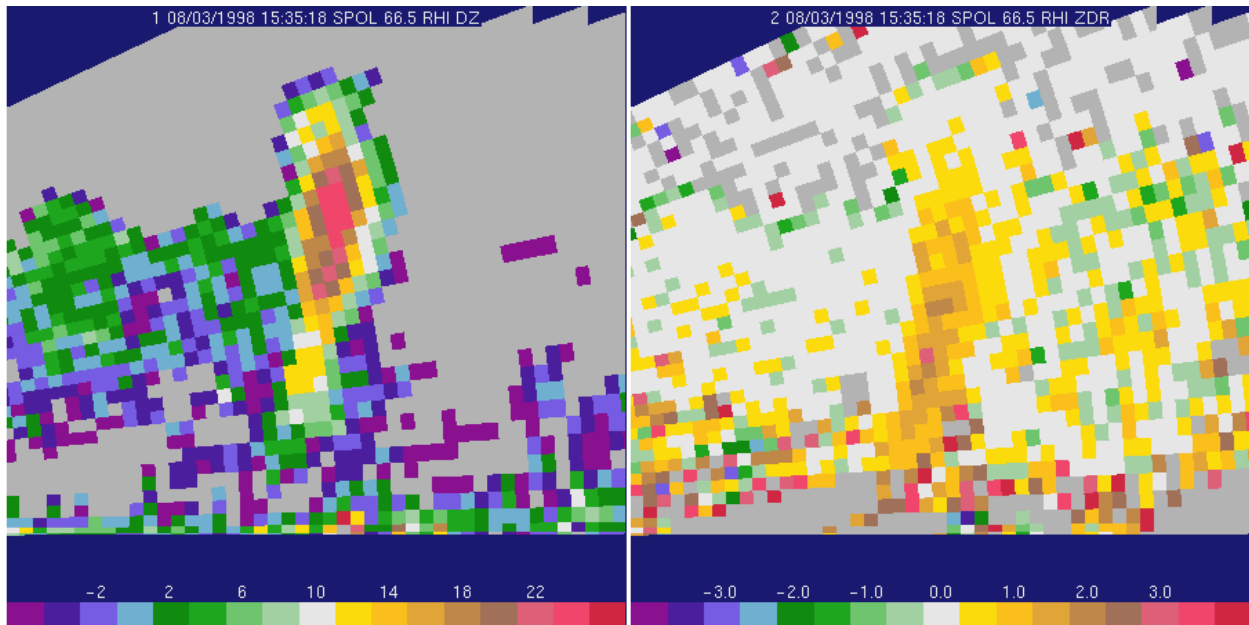


**Fig. 6.** The RHI slice from which the single data points in Fig. 5 were derived.

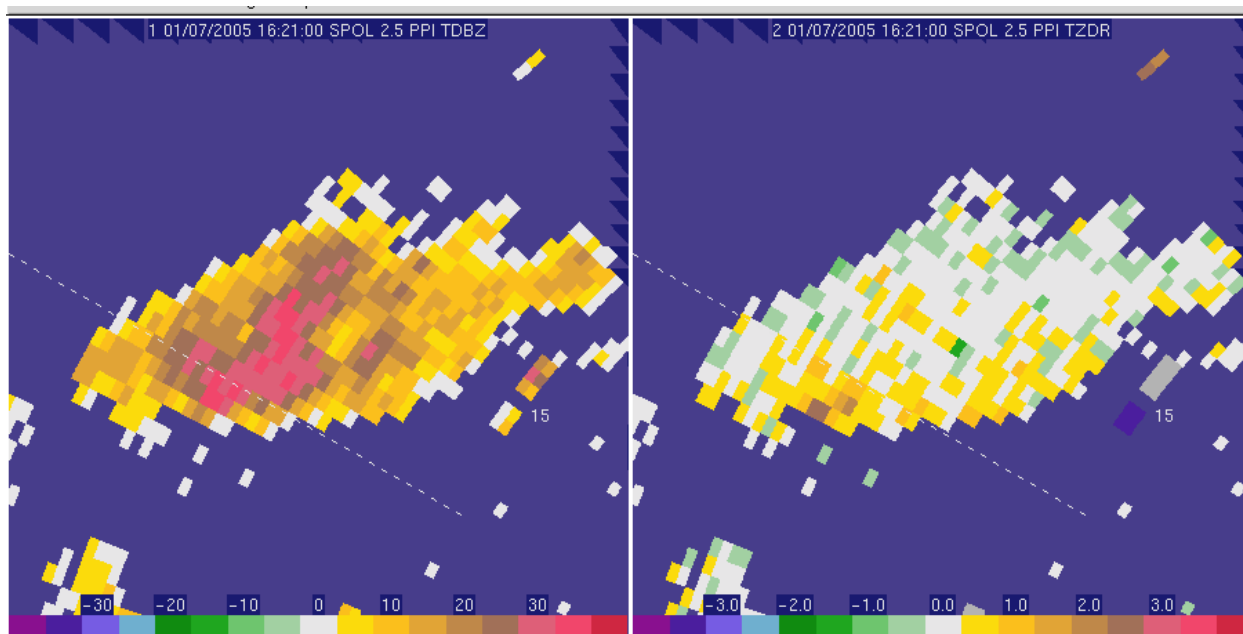


**Fig. 7.** The PPI slice from which Fig. 2 was derived.

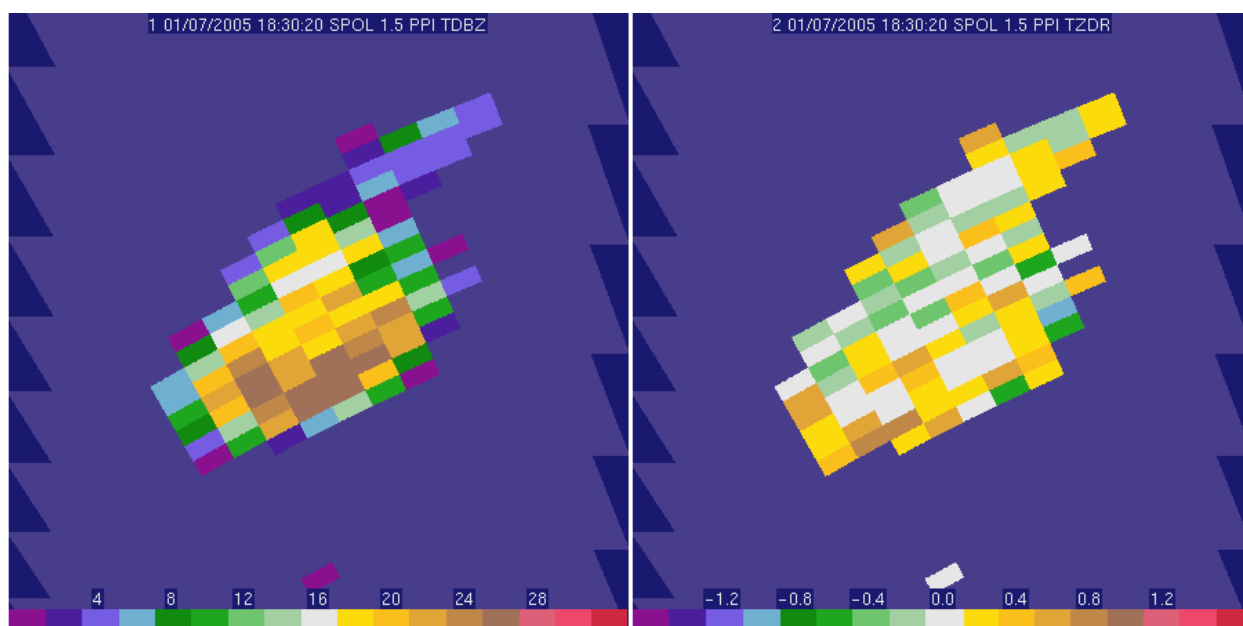


**Fig. 8.** The PPI slice corresponding to the data point in Fig. 4b at about 1826, 1.9km MSL, with  $TZ_{DR}$  of 0.2dB.